iScience

Article

Reduction of intestinal RIPK1 ameliorates HFD-induced metabolic disorders in female mice

Graphical abstract

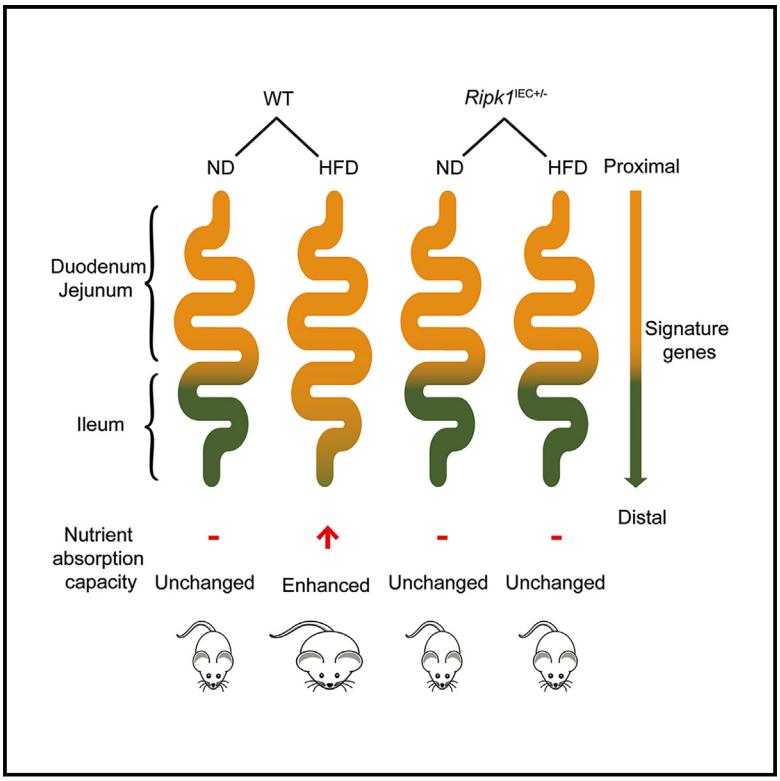

Highlights

- Reducing RIPK1 in the intestine inhibits HFD-induced ileum-to-jejunum shift in female mice
- RIPK1 reduction in the intestine ameliorates HFD-induced metabolic disorders in female mice
- Distinct responses to RIPK1 in the intestine highlight sex-specific metabolic regulation

Authors

Ye Yuan, Xiaomin Hu, Chunguang Guo, ..., Jue Wang, Rui-Ping Xiao, Xiuqin Zhang

Correspondence

xiaor@pku.edu.cn (R.-P.X.), zhangxq@pku.edu.cn (X.Z.)

In brief

Physiology; Pathophysiology

Yuan et al., 2025, iScience *28*, 111906
February 21, 2025
https://doi.org/10.1016/j.isci.2025.111906

CellPress

iScience

CellPress
OPEN ACCESS

Article

Reduction of intestinal RIPK1 ameliorates HFD-induced metabolic disorders in female mice

Ye Yuan,[1,2,7,8] Xiaomin Hu,[1,3,8] Chunguang Guo,[1,2,8] Yihua Xu,[1,2,8] Shihan Li,[1,2] Wei Wen,[1,2,4] Xinli Hu,[1,2] Fanxin Zeng,[1,5] Weiyi Cui,[1,2] Wenli Chen,[1,2] Xueting Sun,[1,2] Ning Hou,[1,2] Jue Wang,[1,2] Rui-Ping Xiao,[1,2,6,*] and Xiuqin Zhang[1,2,7,9,*]

[1]Institute of Molecular Medicine, College of Future Technology, Peking University, Beijing 100871, China
[2]Beijing Key Laboratory of Cardiometabolic Molecular Medicine, Peking University, Beijing 100871, China
[3]Department of Medical Research Center, Peking Union Medical College Hospital, Chinese Academy of Medical Science & Peking Union Medical College, Beijing 100730, China
[4]PKU-Nanjing Institute of Translational Medicine, Nanjing 211800, China
[5]Department of Clinical Research Center, Dazhou Central Hospital, Dazhou 635000, China
[6]State Key Laboratory of Biomembrane and Membrane Biotechnology, Peking-Tsinghua Center for Life Sciences, Beijing 100871, China
[7]National Biomedical Imaging Center, Peking University, Beijing 100871, China
[8]These authors contributed equally
[9]Lead contact
*Correspondence: xiaor@pku.edu.cn (R.-P.X.), zhangxq@pku.edu.cn (X.Z.)
https://doi.org/10.1016/j.isci.2025.111906

SUMMARY

In modern society, excessive nutrient intake from food is a major factor contributing to the development of a series of metabolic disorders and cardiovascular diseases. Further investigation of the mechanisms underlying nutrient absorption in the intestine will help to better understand and develop preventive or therapeutic strategies. In this study, using receptor-interacting protein kinase 1 (*Ripk1*) intestine-specific heterozygous knockout mice (*Ripk1*$^{IEC+/-}$) and high-fat diet (HFD)-feeding mouse model, we report that HFD-induced shift in the transcriptional profile of the ileum toward that of the jejunum, characterized by increased expression of jejunal feature genes in the ileum, are attenuated in *Ripk1*$^{IEC+/-}$ female mice, but not in males. Accordingly, HFD-induced metabolic disorders, including obesity, impaired glucose tolerance, insulin resistance, and dyslipidemia, are significantly ameliorated in the *Ripk1*$^{IEC+/-}$ female mice. These findings demonstrate a new, sex-specific intestinal regulatory mechanism and highlight the critical role of intestinal RIPK1 in regulating HFD-induced metabolic disorders in females.

INTRODUCTION

Obesity is a growing public health concern worldwide. It increases the risk of cardiovascular diseases, type 2 diabetes, cancer, etc.[1] Caloric imbalance is one variable contributing to obesity and metabolic disease, especially excessive caloric intake from food causes energy intake over energy expenditure.[2,3] Other variables also include the involvement of genetic components; genome-wide association studies (GWASs) have identified genes involved in appetite control, such as leptin, and resting energy expenditure, such as FTO (fat mass and obesity associated).[4–7] Nutrients from food are absorbed in the gastrointestinal tract, especially in the small intestine in mammals. Therefore, reducing intestinal excess nutrient absorption would provide protection against obesity and related metabolic diseases.

The duodenum is the first and shortest part of the small intestine, primarily responsible for the further breakdown of food from stomach. The jejunum is distal to the duodenum and the main site of nutrient absorption, especially for the lipid absorption. The ileum, also called the distal intestine, is the final portion of the small intestine and is responsible for absorption of vitamin B_{12}, bile acid, and other remaining nutrients that are not absorbed by jejunum.[8] In line with the functional differences, the proximal and distal intestine have distinct gene expression profiles controlled by specific transcription factors.[9–11] And these distinct gene expression profiles, stem cell proliferation, and differentiation can be altered in high-fat/high-sugar diet-induced obese mice.[12] However, whether different segments of intestine are equally important in the pathogenesis of diet-induced obesity and metabolic disorders, especially between male and female, remains unknown.

Receptor-interacting protein kinase 1 (RIPK1) is an important regulator for both cell death and survival.[13] Global RIPK1 knockout in mice causes early postnatal lethality.[14] Intestinal epithelial specific deletion of RIPK1 also leads to perinatal death in mice due to massive epithelial cell death.[15,16] RIPK1 is also a major player in inflammatory conditions.[17–20] A recent study showed that silencing RIPK1 with antisense oligonucleotides ameliorates high-fat diet (HFD)-induced obesity mainly by reducing the activation of inflammation in adipose tissue and liver in male mice.[21] However, the role of intestinal epithelial

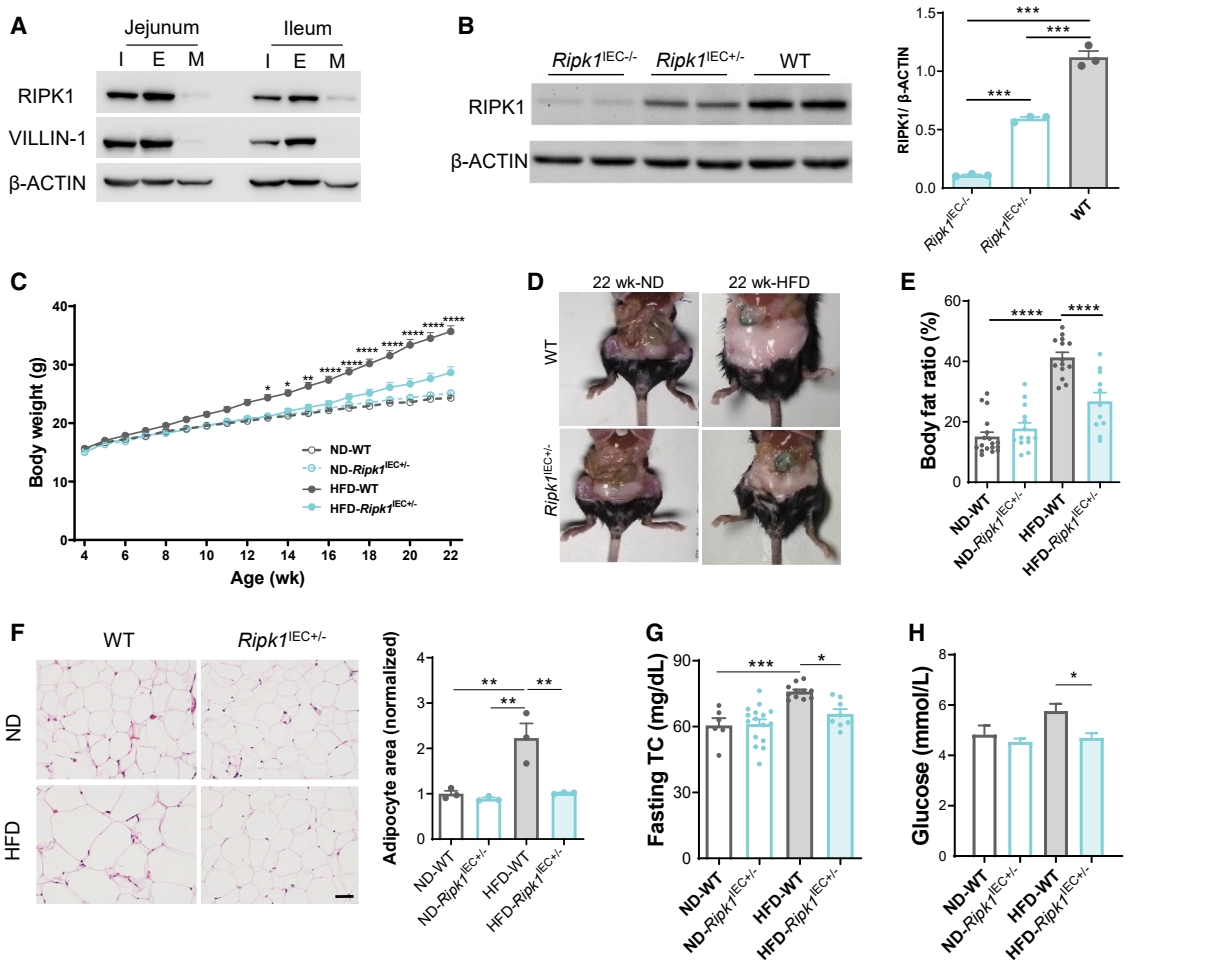

Figure 1. Female *Ripk1*$^{IEC+/-}$ mice resistant to HFD-induced obesity and metabolic disorders

(A) Western blot showing the expression of RIPK1, Villin-1 and β-actin in the epithelium and muscular layer of the jejunum and ileum. I, entire intestine; E, epithelium; M, muscular layer.

(B) Western blot and statistics showing the expression of RIPK1 and β-actin in the jejunums. Statistical tests used were one-way ANOVA with Sidak's multiple comparisons tests.

(C) Body weight (n = 26–46 per group). Statistical tests used were three-way ANOVA with Sidak's multiple comparisons tests.

(D) Representative images of body size and intra-abdominal fat.

(E) Body fat ratio (n = 11–18 per group).

(F) Representative HE-stained sections of visceral white adipose tissue and statistics of adipocyte size. Scale bar, 100 μm.

(G) Overnight fasting plasma TC levels in 22-week-old female mice (n = 6–23 per group).

(H) Overnight fasting blood glucose in 20-week-old female mice (n = 22–33 per group). Statistical tests used were two-way ANOVA with Sidak's multiple comparisons tests [(E), (F, right panel), (G), and (H)]. Data are presented as mean ± SE, *p < 0.05, **p < 0.01, ***p < 0.001, ****p < 0.0001.

RIPK1 in HFD-induced obesity has never been investigated. In this study, we found that knockdown of intestinal epithelial RIPK1 ameliorated HFD-induced obesity in female mice via inhibition of ileal jejunization to prevent excessive nutrients absorption.

RESULTS

Reducing intestinal epithelial RIPK1 attenuates HFD-induced obesity and metabolic disorders in female mice

RIPK1 is essential for intestinal homeostasis,[15,16] it is highly expressed in the small intestinal epithelium (Figure 1A). To test if intestinal epithelial cell (IEC) RIPK1 is involved in HFD-induced obesity, we generated IEC-specific *Ripk1* knockout mice by crossing villin-Cre and *RIPK1*$^{flox/flox}$ mice (Figures S1A–S1D; Figure 1B). As in prior studies,[15,16] we found that almost all of the mice homozygous for IEC *Ripk1*-knockout (*Ripk1*$^{IEC-/-}$) died within one week after birth; only very few *Ripk1*$^{IEC-/-}$ mice could survive to a few weeks, but their body size were much smaller than their wild type (WT) littermates and showed profound villus atrophy (Figure S2A). Heterozygous (*Ripk1*$^{IEC+/-}$) mice survived normally, and on a normal chow diet (ND), the body weight, food intake, intestinal epithelial morphology, cell death, and villus length (Figures S2B–S2E) had no apparent differences compared

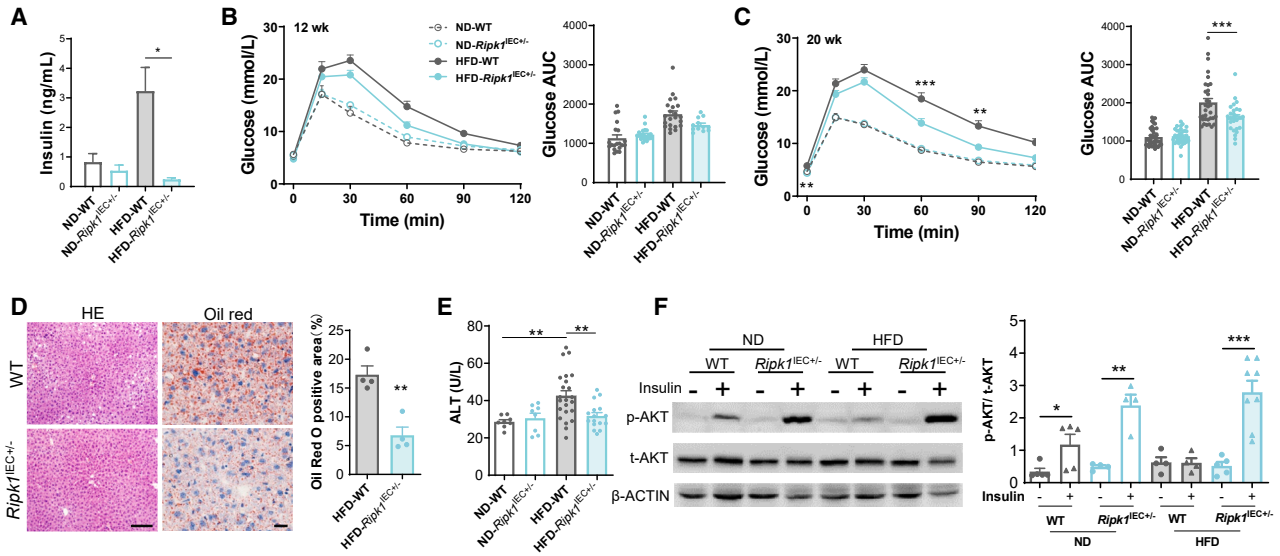

Figure 2. Female *Ripk1*$^{IEC+/-}$ mice resistant to HFD-induced insulin resistance and hepatic steatosis

(A) Overnight fasting plasma insulin levels in 22-week-old female mice (n = 3–9 per group).

(B) Glucose curve and the AUC of ipGTT of 12-week-old female mice (*n* = 12–22 per group).

(C) Glucose curve and the AUC of ipGTT of 20-week-old female mice (*n* = 12–39 per group).

(D) Representative HE and Oil red stained sections of liver, and statistics of Oil red. Scale bar, 100 μm.

(E) Overnight fasting plasma ALT levels (n = 8–23 per group).

(F) Western blots (left) and statistical analysis (right) of total Akt (t-Akt) and phosphorylated Akt (*p*-Akt) at ser473 in the liver (n = 4–8 per group). Statistical tests used were two-way ANOVA with Sidak's multiple comparisons tests [(A), (B, right panel), (C, right panel), and (E)]. Statistical tests used were three-way ANOVA with Sidak's multiple comparisons tests [(B, left panel) and (C, left panel)]. Statistical tests used were unpaired two-tailed Student's *t* test [(D, right panel) and (F)]. Data are presented as mean ± SE, $*p < 0.05$, $**p < 0.01$, $***p < 0.001$.

to those of their WT littermates. However, when the mice were administered a HFD starting at 4 weeks of age, the body weight gain in the female *Ripk1*$^{IEC+/-}$ mice was significantly attenuated relative to female WT (Figure 1C). Surprisingly, the HFD-induced increase in body weight in male *Ripk1*$^{IEC+/-}$ mice were comparable with the male WT mice (Figure S3A). In accordance with the body weight change in female mice, after 18 weeks of HFD feeding, *Ripk1*$^{IEC+/-}$ mice had less visceral fat mass (Figure 1D), significantly lower body fat ratio (Figure 1E), and smaller visceral adipocytes (Figure 1F) compared to female WT mice. Moreover, compared to WT female mice, female *Ripk1*$^{IEC+/-}$ mice displayed reduced levels of fasting blood total cholesterol (TC) (Figure 1G) and fasting glucose (Figure 1H) after 18 weeks of HFD feeding.

Obesity is associated with increased insulin resistance. We found that HFD-induced increase in serum insulin was reduced in *Ripk1*$^{IEC+/-}$ female mice (Figure 2A); furthermore, the deteriorated glucose tolerance induced by HFD was also ameliorated in the female *Ripk1*$^{IEC+/-}$ mice when tested at both 12 weeks (HFD-feeding for 8 weeks) and 20weeks (HFD feeding for 16 weeks), respectively (Figures 2B–2C). Once again, the HFD-induced deterioration of glucose tolerance in the male *Ripk1*$^{IEC+/-}$ mice was comparable to that in WT male mice in multipole tests (Figure S3B). Because obesity frequently presents with fatty liver, we then investigated the influence of reduced intestinal epithelial RIPK1 on liver steatosis. Along with the reduced body weight, the liver size was smaller (Figure S4A) and the liver weight was significantly lower in female *Ripk1*$^{IEC+/-}$ mice fed with HFD (Figure S4B). Hematoxylin-eosin (HE) and Oil red staining of liver sections showed that fat deposition in HFD-fed female *Ripk1*$^{IEC+/-}$ mice was fewer than HFD-fed WT mice (Figure 2D), and the alanine aminotransferase (ALT) was lower in HFD-fed female *Ripk1*$^{IEC+/-}$ mice than in HFD-fed WT mice (Figure 2E). However, the cell death indicated by cleaved caspase-3 immunohistochemical staining (Figure S4C), inflammatory cell infiltration indicated by CD45 immunohistochemical staining (Figure S4D), and fibrosis indicated by Masson staining (Figure S4E) in the liver were not different between HFD-fed WT and *Ripk1*$^{IEC+/-}$ female mice. Nevertheless, the fat deposition was not different between HFD-fed male *Ripk1*$^{IEC+/-}$ and WT mice in the liver (Figure S3C). In addition, insulin sensitivity evidenced by insulin-stimulated Akt phosphorylation (*p*-Akt) was clearly attenuated in the livers of the HFD-fed female WT mice, but not affected by HFD in *Ripk1*$^{IEC+/-}$ mice (Figure 2F). All the above results demonstrated that reducing intestinal RIPK1 effectively attenuated HFD-induced obesity and related metabolic disorders in female mice, suggesting that intestinal response to HFD maybe had a sex difference. Based on above observations, in the subsequent studies, we focused on revealing the function of intestinal RIPK1 in HFD-induced obesity in female mice.

HFD induces ileal jejunization in female mice

Studies showed that IEC proliferation and villi elongation induced by HFD or high-fat/high-sugar diet contribute to obesity in male mice.[12,22] However, the villi elongation (Figure S5A) and

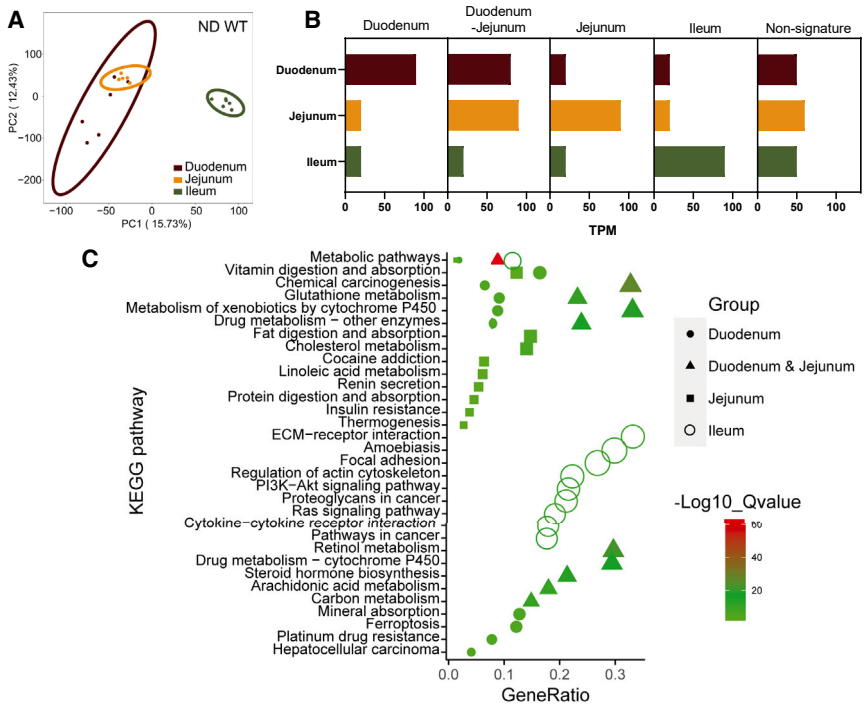

Figure 3. Identification of signature genes for each segment of the small intestine

(A) PCA score plots of 22, 493 genes expression data in various segments of the small intestine of 22-week WT mice fed with ND.

(B) Signature gene screening in different segments of the small intestine.

(C) KEGG pathway enrichment analysis of gene expression in different segments of the small intestine from 22-week ND WT mice.

epithelial cell proliferation (Figure S5B) did not differ significantly between *Ripk1*$^{IEC+/-}$ and WT mice fed with ND or HFD in females. Since RIPK1 is important in regulating cell death, we did TUNEL staining in the ileum of HFD-fed female mice, and the results showed that there was no significant difference in TUNEL-positive cells between WT and *Ripk1*$^{IEC+/-}$ mice (Figure S5C). Therefore, epithelial cell proliferation and cell death are not likely the underlying mechanisms of the improved metabolic phenotypes in HFD-fed *Ripk1*$^{IEC+/-}$ female mice.

To gain insights into the systematic changes in the intestine induced by HFD in the female mice, we used RNA-seq to profile the transcriptome of different segments of the intestine from female WT mice on ND and HFD. Principal component analysis (PCA) revealed that under ND feeding, the transcriptional profiles of the duodenum and jejunum, portions of the proximal small intestine, were similar; while the transcriptional profile of ileum was distinct from that of the proximal small intestine (Figure 3A). Using a 2-fold change and an adjusted *p* value of 0.05 as threshold comparing transcriptomes of duodenum vs. jejunum, duodenum vs. ileum, and jejunum vs. ileum, we defined 480, 941, 50, and 777 genes that were enriched in the duodenum, duodenum-jejunum, jejunum, and ileum as their signature genes, respectively (Figure 3B; Table S1). Pathway enrichment analysis showed that duodenal and/or jejunal signature genes are involved mainly in signaling pathways related to nutrient digestion and absorption, which was consistent with their main function (Figure 3C). In contrast to the absorption related signaling pathways, the ileal signature genes are involved largely in ECM-receptor interaction, focal adhesion, and immune response related pathways; these are also consistent with the main function of the ileum (Figure 3C).

2Interestingly, after HFD feeding, the transcriptional profiles of the duodenum and jejunum showed no obvious change, but the transcriptional profile of the ileum was shifted toward those of the duodenum and jejunum in WT mice (Figure 4A), indicating that the ileum was the portion of the intestine affected the most by HFD at transcriptional level. Consistent with this shifted direction, the HFD-upregulated genes in the ileum were mainly enriched in major nutrient digestion and absorption pathways (Figure 4B), while the downregulated genes were largely involved in steroid biosynthesis, terpenoid biosynthesis, nitrogen metabolism, and immune response related pathways (Figure 4B). Further gene set enrichment analysis (GSEA) of signature genes revealed that the transcriptome of the ileum of HFD-fed WT mice was close to that of the ND-fed jejunum and duodenum-jejunum rather than ND-fed ileum (Figure 4C). Thus, many jejunal signature genes were upregulated by HFD in the ileum, while many ileal signature genes were downregulated, after HFD feeding (Figure 4D; Table S1). Furthermore, the jejunal signature genes that gained in the ileum after HFD-feeding are mainly involved in nutrient absorption and metabolism (Figure 4E), while the downregulated signature genes in the ileum are largely related to steroid biosynthesis, terpenoid biosynthesis, sulfur metabolism, and nitrogen metabolism pathways (Figure 4E). These results demonstrated that HFD induces the ileum to gain the expression of jejunal signature genes and lose ileal signature genes at the transcriptional level. We termed these changes 'ileal jejunization'.

Reducing intestinal RIPK1 counteracts HFD-induced ileal jejunization and nutrient absorption in female mice

To understand whether the improved metabolic phenotypes of reducing intestinal RIPK1 in HFD-fed female mice is related with ileal jejunization, we further analyzed the transcriptomes of different segments of the *Ripk1*$^{IEC+/-}$ intestine in the ND or HFD-fed group (Figure 5A), and also those between *Ripk1*$^{IEC+/-}$ and WT mice on ND or HFD (Figure 5B). Similar to the WT intestine, the transcriptomes of *Ripk1*$^{IEC+/-}$ duodenum and jejunum shared high degree of similarity, while being quite different from that of ileum under ND conditions (Figure 5A, left). Remarkably, the HFD-induced shift of ileal transcriptome that seen in WT

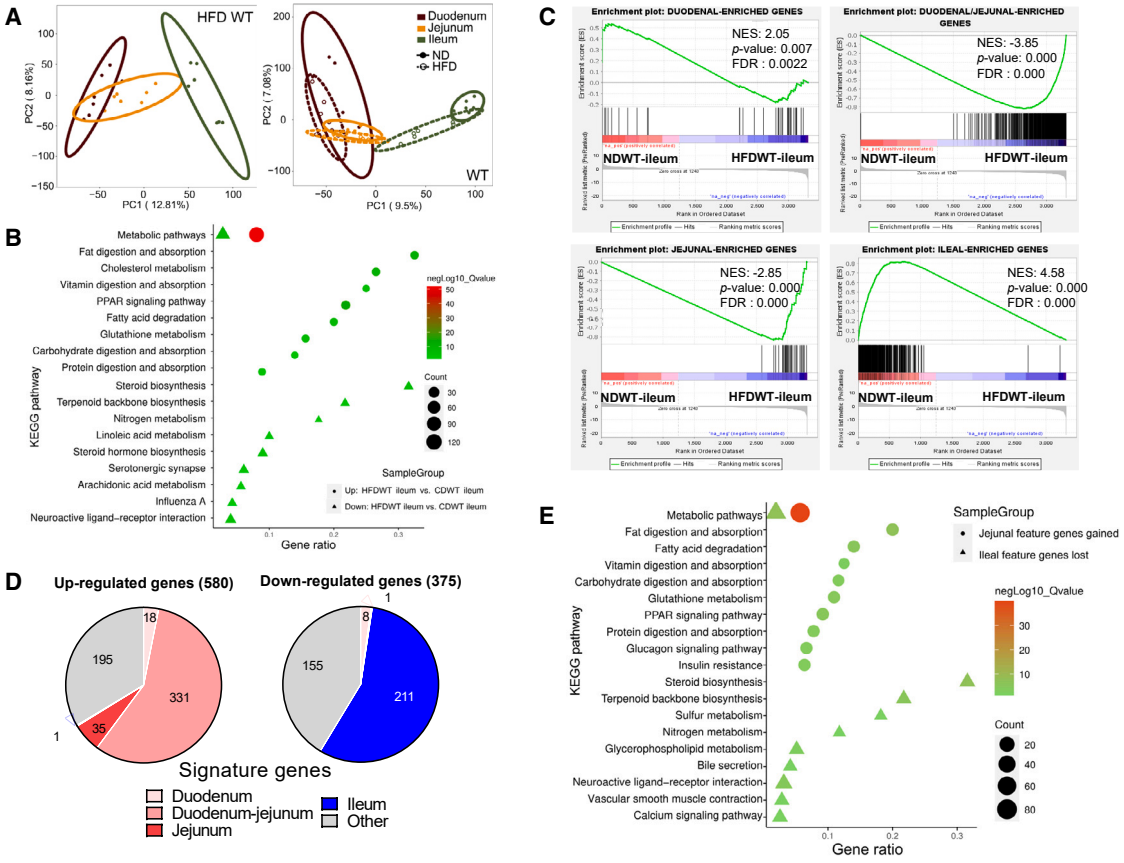

Figure 4. HFD induces ileal jejunization in female mice

(A) PCA score plots of 22, 493 genes expression data in the small intestine of 22-week female WT mice fed with ND or HFD.

(B) KEGG pathway enrichment analysis of upregulated or downregulated genes in ileum of WT mice after HFD-feeding.

(C) GSEA was performed with RNA-seq data from the ileum of 22-week-old female WT mice fed with ND or HFD. Transcripts identified as signature genes in the duodenum (top left), duodenum/jejunum (top right), jejunum (bottom left), or ileum (bottom right) of ND WT mice were used as reference gene sets.

(D) HFD-induced changes of gene expression in ileum of WT mice compare to ND-fed ileum.

(E) KEGG pathway enrichment analysis of upregulated or downregulated signature genes in ileum of WT mice after HFD-feeding.

mice (Figure 4A) was blocked in *Ripk1*$^{IEC+/-}$ mice (Figure 5A, right). The difference between HFD-fed WT and *Ripk1*$^{IEC+/-}$ mice was more evident when the transcriptomes of different intestinal segments and diets were analyzed together (Figure 5B). Compared to HFD-fed WT ileum, nutrient absorption and metabolism signaling pathways were downregulated, while the immune pathways were upregulated in the HFD-fed *Ripk1*$^{IEC+/-}$ ileum (Figure 5C). The jejunal feature genes as shown in the Figure 5D were downregulated compared to HDF WT mice and ileal marker genes were upregulated, signifying that the transcriptional profile of HFD-fed *Ripk1*$^{IEC+/-}$ mice in the ileum resembled the ileum of ND WT mice and not the jejunum. Consistently, 2 h after BODIPY-FA gavage, the lipid uptake in the jejunum and ileum did not differ between ND WT and ND *Ripk1*$^{IEC+/-}$, but the lipid uptake was markedly increased in the ileum of WT mice in HFD group, while the lipid uptake in HFD-treated *Ripk1*$^{IEC+/-}$ mice was similar to those of the mice on ND groups (Figure 5E). Measuring plasma TG levels after oral olive oil gavage is a commonly used method to assess the capacity for intestinal lipid absorption. Indeed, the serum TG level was significantly lower in the HFD-fed *Ripk1*$^{IEC+/-}$ mice than HFD-fed WT mice after gavage of olive oil (Figure 5F).

Furthermore, quantitative reverse transcription polymerase chain reaction (qRT-PCR) confirmed that nutrient uptake-related ileal jejunization genes were only dramatically upregulated in the ileum of HFD-treated WT mice, but not in the HFD-treated *Ripk1*$^{IEC+/-}$ ileum when compared to ND-fed mice (Figure 6A). Accordantly, the proximal intestinal marker genes were upregulated while distal intestinal marker genes were downregulated in the ileum of HFD-treated WT mice, but not in the HFD-treated *Ripk1*$^{IEC+/-}$ ileum (Figure 6A). However, such changes were absent in the ileum of HFD-fed male mice (Figure 6B).

To confirm if the different metabolic phenotypes between HFD-fed male and female mice were related to the levels of RIKP1 expression, the expression of *Ripk1* in the intestine was assessed by q-PCR. At postnatal day 1 (P1) and week 4, *Ripk1* expression in the intestines of *Ripk1*$^{IEC+/-}$ mice was significantly lower than that in their WT controls in both males and females (Figures 7A and 7B). Surprisingly, at 8 weeks, *Ripk1* expression in the intestines of *Ripk1*$^{IEC+/-}$ male mice was comparable to

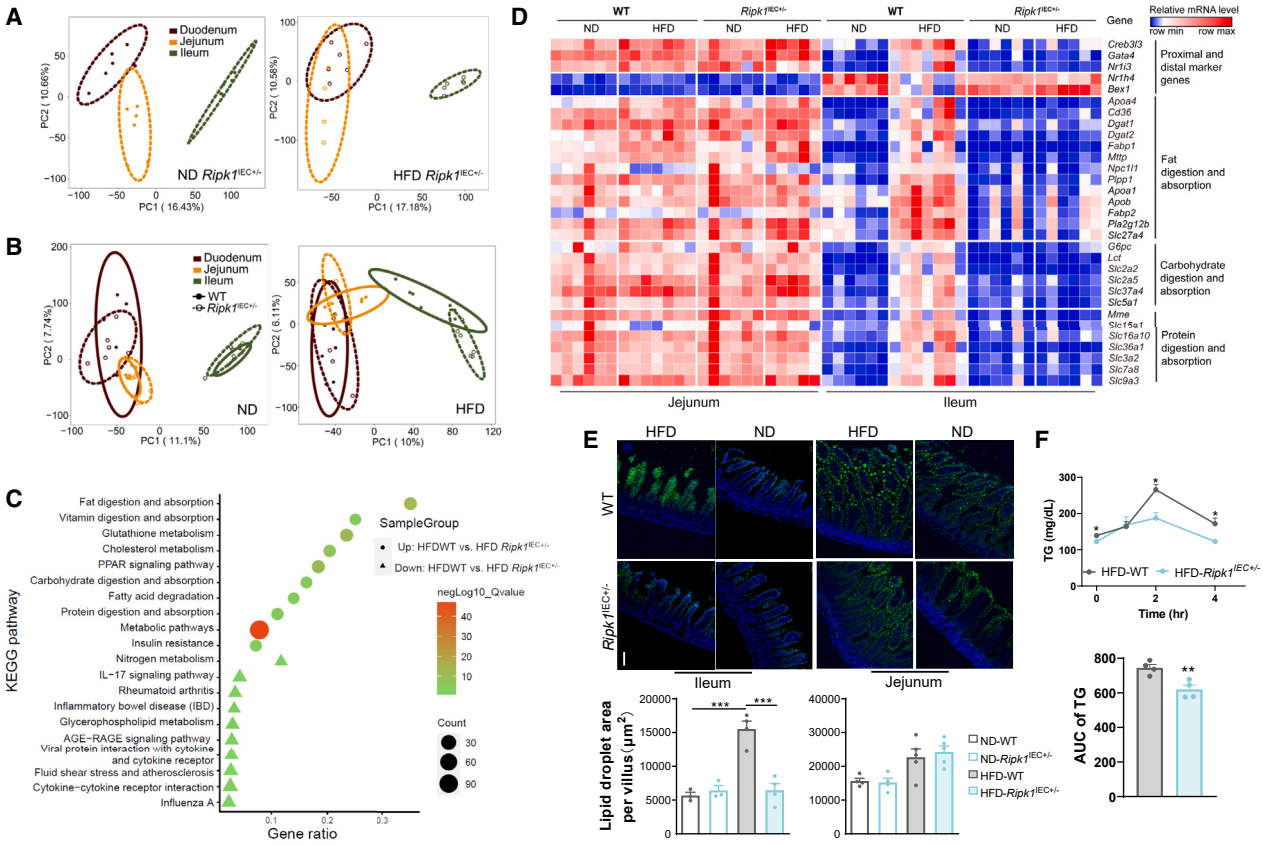

Figure 5. Reducing intestinal RIPK1 inhibits ileal jejunization and lipid absorption induced by HFD in female mice

(A) PCA score plots of 22,493 gene expression data in the small intestine of *Ripk1*$^{IEC+/-}$ mice.

(B) PCA score plots of 22,493 gene expression data in the small intestine of WT and *Ripk1*$^{IEC+/-}$ mice.

(C) KEGG pathway enrichment analysis of differentially expressed genes in ileum of WT and *Ripk1*$^{IEC+/-}$ mice after HFD-feeding.

(D) Heatmap showing the transcription of marker genes and nutrient absorption-related genes in the jejunum and ileum of mice with different genotypes and diets.

(E) Representative images and statistics of the lipid uptake in the jejunum and ileum 2 h after BODIPY-FA gavage. Green fluorescence represents lipids. Scale bar, 100 μm. Statistical tests used were two-way ANOVA with Sidak's multiple comparisons tests.

(F) Serum TG curve and the AUC of the oil gavage test in 18-week-old female mice (n = 4–6 per group). Data are presented as mean ± SE, $^{*}p < 0.05$, unpaired *t-test*.

their WT controls, while *Ripk1* expression in the intestines of *Ripk1*$^{IEC+/-}$ female mice remained lower than in WT female mice (Figures 7A and 7B). Furthermore, at 22 weeks of age, *Ripk1* expression in the ileum of both ND- and HFD-fed *Ripk1*$^{IEC+/-}$ female mice was significantly lower than in WT mice (Figure 7C). In contrast, *Ripk1* expression in the ileum of *Ripk1*$^{IEC+/-}$ male mice did not differ significantly from that of WT mice in either ND- or HFD-fed conditions (Figure 7D) These results may explain why epithelial cell specific-RIPK1 knockdown is more effective in ameliorating the HFD-induced metabolic disorders in female mice, suggesting that ileal jejunization might be a fundamental mechanism for ileal functional adaptation in response to HFD stimuli in female mice, and confirmed that RIPK1 playing a critical role in such intestinal adaptation.

Ileal jejunization and absorption elevation occurs before the onset of obesity in HFD-fed female mice

Studies have found that 1-week HFD feeding can significantly increase intestinal epithelium lipid absorption in mice.[23] To further elucidate whether ileal jejunization also occurred prior to obesity, we examined the ileal jejunization-related gene expression in the ileum of female mice before the onset of obesity (fed with HFD for 2 weeks), and compared with those of ND-fed WT mice (Figure 8A). qRT-PCR showed that the expression of ileal jejunization-related nutrient absorption genes was increased significantly in the ileum of HFD-fed WT mice, while these changes were suppressed in the HFD-fed *Ripk1*$^{IEC+/-}$ mice (Figure 8B). Fasting plasma TG and TC were also significantly increased in the WT mice than in *Ripk1*$^{IEC+/-}$ mice after 2 weeks of HFD-feeding (Figure 8C). Furthermore, the TG level 2 h after olive oil gavage was higher in HFD WT mice compared with HFD *Ripk1*$^{IEC+/-}$ mice (Figure 8D). To test whether the HFD-induced changes in the female mice are dependent on RIPK1 kinase activity, we treated HFD-fed WT female mice with the RIPK1 kinase inhibitor Nec-1s. We found that Nec-1s had no significant effect on HFD-induced changes in body weight (Figure S6A), serum TG and TC (Figure S6B), and gene expression (Figure S6C), suggesting that RIPK1-kinase activity is possibly not necessary for

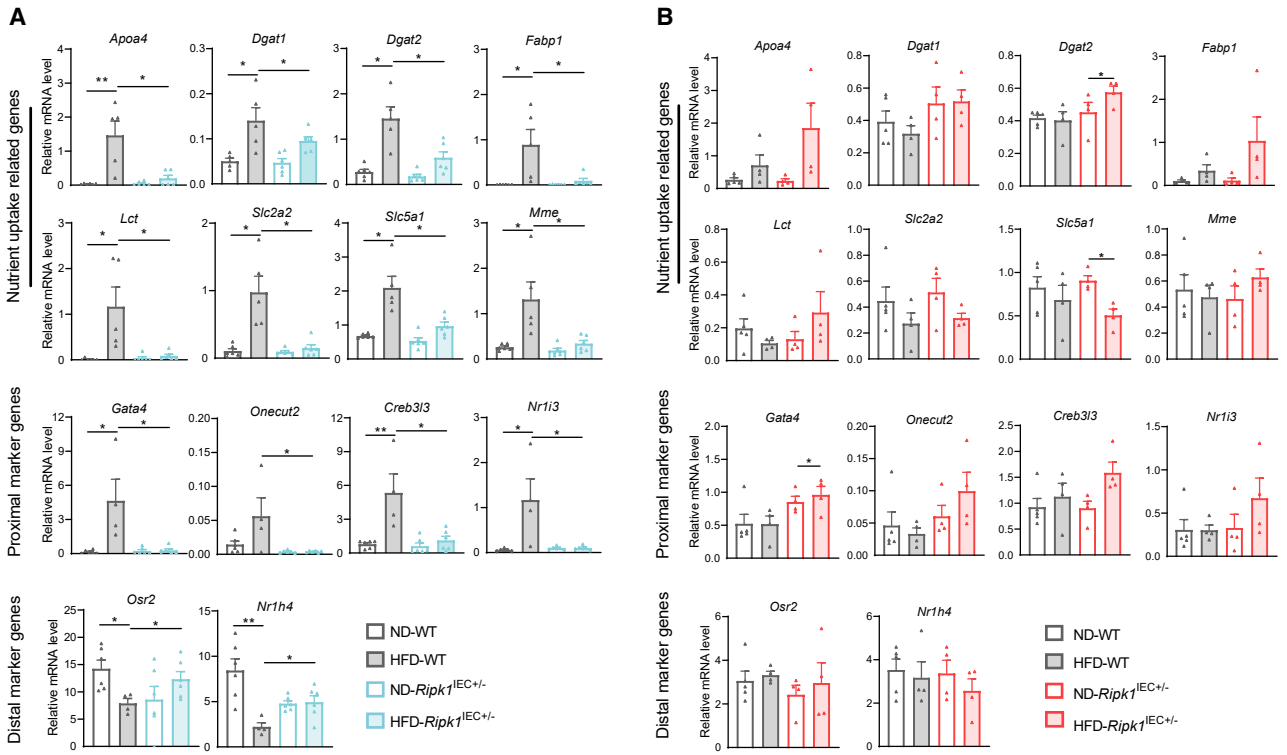

Figure 6. HFD-induced ileal jejunization is absent in male mice

(A) mRNA expression levels of ileal jejunization and nutrient uptake related genes, proximal and distal intestinal marker genes in the ileum of 22-week-old female mice (n = 4–6 per group).

(B) mRNA expression levels of ileal jejunization and nutrient uptake related genes, proximal and distal intestinal marker genes in the ileum of 30-week-old male mice (n = 4–6 per group). Statistical tests used were two-way ANOVA with Sidak's multiple comparisons tests [(A) and (B)]. Data are presented as mean ± SE, $^{*}p < 0.05$, $^{**}p < 0.01$, $^{***}p < 0.001$.

these changes. These results confirmed that an HFD-induced ileal jejunization and an increase in nutrient absorption occurred before the onset of obesity. And further confirmed the regulatory effect of intestinal RIPK1 in ileal jejunization in female mice.

Taken together, our findings indicated that the HFD-induced increase in intestinal absorption takes place mainly in the ileum of female mice. The abundance of intestinal RIPK1 plays important role in this process. Reducing RIPK1 in the intestine can effectively prevent obesity and metabolic disorders caused by HFD.

DISCUSSION

Obesity is closely related to energy intake from food, especially in women.[2,24–26] Studies have shown that an HFD promotes obesity.[27,28] HFD also activates the hedonic center to increase food intake, which leads to excessive energy intake and, ultimately, obesity.[29] All these results indicate that systemic changes related to excess energy intake contribute to the progression of obesity. In this study, we demonstrated that the ileum, the distal intestine, plays a dominant role in HFD-induced obesity and related metabolic disorders in female mice, and the amount of RIPK1 in the IEC is a critical mediator during these processes.

Most investigations of fat absorption in the intestine were conducted several decades ago. Using intestinal intubation, Borgstrom et al. showed that the jejunum is the main site of fat absorption in humans.[30] An acute oil gavage study in rats further confirmed that the jejunum is the main site of fat absorption. When faced with larger amounts of ingested fat, absorption spills over from the jejunum to the ileum.[31] This evidence was also confirmed in healthy individuals and in patients who underwent various degrees of intestinal resection.[32] These findings indicated that the jejunum is the predominant site for fat absorption, and that the ileum contributes when fat has exceeded the ability of jejunum to absorb it. In 1954, Kremen et al. performed surgeries to remove the distal or proximal intestine in dogs. They found that the body weight loss happens immediately after removing 50% of the proximal intestine, but that body weight gradually was regained 10 weeks after the surgery and returned to the pre-operative weight at 24 weeks post-surgery.[33] However, when 50% of the distal intestine was removed, the initial body weight loss was similar to that seen after removing the 50% of proximal intestine, but the dogs did not regain body weight after 24 weeks.[33] These results indicate that the ileum has more flexibility or adaptability in response to nutrient ingestion. Nevertheless, the underlying mechanism for such changes in the ileum remains unknown. In this study, we found that when female mice

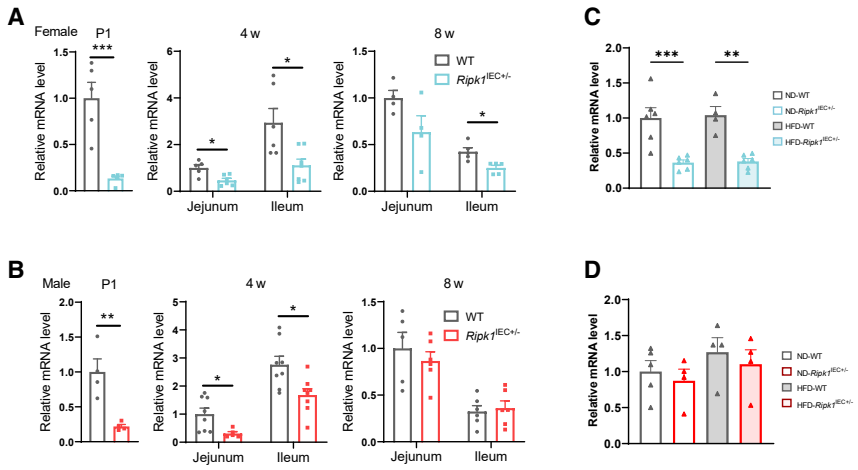

Figure 7. RIPK1 mRNA expression in the intestines of male and female mice

(A) mRNA expression levels of Ripk1 in the intestine of ND-fed WT and Ripk1IEC−/− female mice.
(B) mRNA expression levels of *Ripk1* in the intestine of ND-fed WT and *Ripk1*$^{IEC-/-}$ male mice.
(C) mRNA expression levels of *Ripk1* in the ileum of ND- or HFD-fed WT and *Ripk1*$^{IEC-/-}$ female mice.
(D) mRNA expression levels of *Ripk1* in the ileum of ND- or HFD-fed WT and *Ripk1*$^{IEC-/-}$ male mice. Statistical tests used were unpaired two-tailed Student's *t* test [(A) and (B)]. Statistical tests used were two-way ANOVA with Sidak's multiple comparisons tests [(C) and (D)]. Data are presented as mean ± SE, $*p < 0.05$, $**p < 0.01$, $***p < 0.001$.

are exposed to an HFD, the ileum acquires more jejunal-like features and increases its adaptability for nutrients absorption, and the amount of intestinal RIPK1 is important regulator for this process.

Besides differences in absorptive ability between the proximal and distal intestine, recent studies have revealed differences in their gene expression.[9,10,12,34] GATA4, a proximal intestinal marker gene, is critical for establishing and maintaining the jejunal-ileal epithelial identities.[9,10] GATA4 regulates a panel of absorptive gene expression, especially those involved in lipid metabolism. Mice lacking intestinal epithelial-GATA4 dramatically downregulated genes involved in lipid and cholesterol uptake, transport and processing in the jejunum, significantly reduced cholesterol and dietary fat absorption.[9] On the other hand, the transcriptional identity of jejunum and duodenum is induced in the ileum when GATA4 is ectopically expressed in the ileum.[11] In this study, we found that HFD significantly upregulated GATA4 and jejunal-character genes in the ileum and lipid uptake was also increased in the HFD-fed ileum. However, these upregulations were prevented in the ileum of *Ripk1*$^{IEC+/-}$ female mice. These results indicate that HFD-induced ileal jejunization is the basis of the increase in adaptive absorption in the ileum, and that intestinal RIPK1 is a key controller for this adaptation in female, but not in male mice, revealing a sex-differentiated mechanism in HFD-induced obesity.

RIPK1 is a star molecule in regulating cell fate, immune response, and inflammatory disease, and has been extensively studied.[13,19,35,36] One recent study found that globally silencing of RIPK1 suppresses HFD-induced adipose tissue and liver inflammation, and consequently obesity in male mice.[21] We observed an improvement in HFD-induced metabolic disorders in female *Ripk1*$^{IEC+/-}$ mice, but not in male *Ripk1*$^{IEC+/-}$ mice. Additionally, we noted that *Ripk1* expression in the small intestines of *Ripk1*$^{IEC+/-}$ male mice was significantly lower than their WT controls at both newborn and 4 weeks of age. However, *Ripk1* expression in the intestines was no longer different between *Ripk1*$^{IEC+/-}$ and WT male mice at 8 weeks and 30 weeks of age. The difference in RIPK1 levels may explain the phenotypic differences between *Ripk1*$^{IEC+/-}$ males and females following HFD feeding. Further investigation is needed into the underlying mechanisms by which RIPK1 expression changes with age in *Ripk1*$^{IEC+/-}$ male mice, as well as the mechanisms by which RIPK1 regulates HFD-induced changes in gene expression. In particular, it is crucial to determine whether

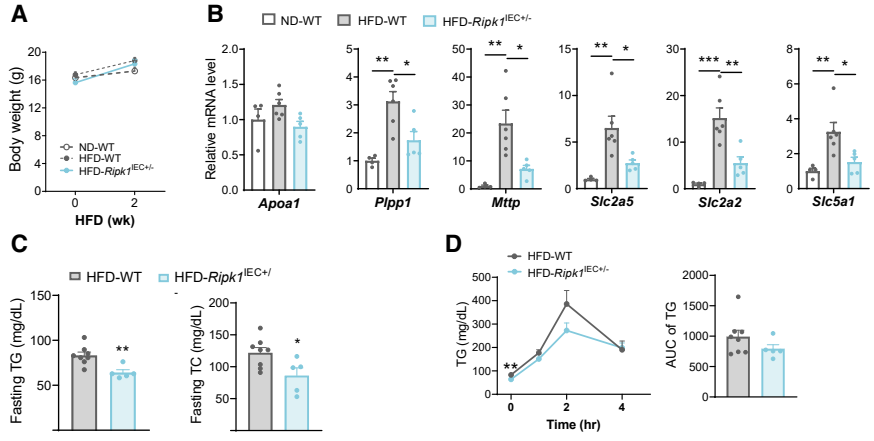

Figure 8. Ileal jejunization is induced by HFD prior to the onset of obesity

(A) Body weight of female mice (n = 4–6 per group).
(B) mRNA expression levels of nutrient absorption-related genes in the ileum (n = 5–8 per group).
(C) Overnight fasting plasma TG and TC levels of female mice (n = 5–8 per group).
(D) Plasma TG curve and the AUC of the oil gavage test in female mice (n = 4–6 per group).
Statistical tests used were unpaired two-tailed Student's *t* test [(A), (C) and (D)]. Statistical tests used were one-way ANOVA with Sidak's multiple comparisons tests [(B)]. Data are presented as mean ± SE, $*p < 0.05$, $**p < 0.01$, $***p < 0.001$.

RIPK1 knockdown affects gene expression by altering gut microbiota composition and activity, considering the sex differences in microbiota.[37,38] Our findings add a potential sex preference mechanism for RIPK1 in mediating obesity related to an HFD. Disrupting RIPK1 may act by both anti-inflammatory and inhibiting absorption, with preference to different genders, to exert its beneficial effects on HFD-induced obesity and metabolic disorders.

Taken together, our findings not only discovered that ileal jejunization is the major initiator of HFD-induced obesity in female mice, but also highlighted a new function of intestinal RIPK1 in regulating metabolic disease with sex-preferential mechanism. These results provide the potential for targeting RIPK1 in the prevention or treatment of diet-related obesity and metabolic disorders.

Limitations of the study

In this study, we have revealed a new, sex-specific regulatory mechanism of intestinal RIPK1 in regulating HFD-induced metabolic disorders in female mice. However, the depth of underlying mechanisms by which intestinal RIPK1 respond to HFD are not yet fully understood. Comprehensive *in vivo* and *in vitro* experiments are needed to explore the molecular signaling pathways in future studies. The current findings are based on an HFD-induced mouse model, so it is critical to study whether such sex differences are present in humans. For this, collaboration with clinical scientists to collect human samples for further investigation is essential.

RESOURCE AVAILABILITY

Lead contact

Requests for further information and resources should be directed to and will be fulfilled by the lead contact, Xiuqin Zhang (zhangxq@pku.edu.cn).

Materials availability

The materials used and generated in this study are available from the lead contact with a completed material transfer agreement.

Data and code availability

- Data: All data reported in this article will be shared by the lead contact upon request. RNA-Seq data have been deposited at NCBI Gene Expression Omnibus (http://www.ncbi.nlm.nih.gov/geo) and are publicly available as of the date of publication. Accession numbers are listed in the key resources table.
- Code: This article does not report the original code.
- Any additional information required to reanalyze the data reported in this paper is available from the lead contact upon reasonable request.

ACKNOWLEDGMENTS

We thank Dr. Jon Moon for editing the English, Dr. Shu-Yong Lin for constructive comments on this study. This work was supported by the National Natural Science Foundation of China (81471063, 81970690), and National Key Research and Development Program of China (2018YFA0801405, 2018YFA0507600).

AUTHOR CONTRIBUTIONS

Y.Y. conceived the project, designed and performed experiments, analyzed and interpreted data, made the figures, and wrote the manuscript; X.H. designed and performed experiments, analyzed data, made the figures, and wrote the manuscript; C.G., W.W., Y.X., F.Z., W.C., W.C., S.L., X.S., and N.H. performed experiments; J.W. analyzed the data and edited the manuscript; X.H. created *Ripk1-Loxp* mice, provided technical support, and edited the manuscript; R.-P.X. worked on project design and data interpretation; X.Z. conceived the project, designed experiments, interpreted data, and wrote the manuscript.

DECLARATION OF INTERESTS

The authors declare no competing interests.

STAR★METHODS

Detailed methods are provided in the online version of this paper and include the following:

- KEY RESOURCES TABLE
- EXPERIMENTAL MODEL AND STUDY PARTICIPANT DETAILS
  - Mice
- METHOD DETAILS
  - Blood glucose, plasma insulin and ALT measurement
  - Glucose tolerance test
  - Lipid absorption assay
  - Tissue sample collection
  - Histology and immunohistochemistry
  - TUNEL staining
  - Western blotting
  - RNA-seq analysis
  - Screening signature genes
  - qRT-PCR analysis
- QUANTIFICATION AND STATISTICAL ANALYSIS

SUPPLEMENTAL INFORMATION

Supplemental information can be found online at https://doi.org/10.1016/j.isci.2025.111906.

Received: June 22, 2024
Revised: November 27, 2024
Accepted: January 23, 2025
Published: January 27, 2025

REFERENCES

1. Adams, K.F., Schatzkin, A., Harris, T.B., Kipnis, V., Mouw, T., Ballard-Barbash, R., Hollenbeck, A., and Leitzmann, M.F. (2006). Overweight, Obesity, and Mortality in a Large Prospective Cohort of Persons 50 to 71 Years Old. N. Engl. J. Med. *355*, 763–778.
2. Hall, K.D., Heymsfield, S.B., Kemnitz, J.W., Klein, S., Schoeller, D.A., and Speakman, J.R. (2012). Energy balance and its components: implications for body weight regulation. Am. J. Clin. Nutr. *95*, 989–994. https://doi.org/10.3945/ajcn.112.036350.
3. Levitsky, D.A., Sewall, A., Zhong, Y., Barre, L., Shoen, S., Agaronnik, N., LeClair, J.-L., Zhuo, W., and Pacanowski, C. (2019). Quantifying the imprecision of energy intake of humans to compensate for imposed energetic errors: A challenge to the physiological control of human food intake. Appetite *133*, 337–343.
4. Dina, C., Meyre, D., Gallina, S., Durand, E., Körner, A., Jacobson, P., Carlsson, L.M.S., Kiess, W., Vatin, V., Lecoeur, C., et al. (2007). Variation in FTO contributes to childhood obesity and severe adult obesity. Nat. Genet. *39*, 724–726. https://doi.org/10.1038/ng2048.
5. Frayling, T.M., Timpson, N.J., Weedon, M.N., Zeggini, E., Freathy, R.M., Lindgren, C.M., Perry, J.R.B., Elliott, K.S., Lango, H., Rayner, N.W., et al. (2007). A common variant in the FTO gene is associated with body mass index and predisposes to childhood and adult obesity. Science *316*, 889–894. https://doi.org/10.1126/science.1141634.

6. van der Klaauw, A.A., and Farooqi, I.S. (2015). The hunger genes: pathways to obesity. Cellule *161*, 119–132. https://doi.org/10.1016/j.cell.2015.03.008.

7. Argente, J., and Tena-Sempere, M. (2023). Clinical and Molecular Features of Patients With Leptin and Leptin Receptor Deficiency: Lessons of 25 Years of Research. J. Clin. Endocrinol. Metab. *109*, e424–e425. https://doi.org/10.1210/clinem/dgad353.

8. Jiang, C., Xie, C., Lv, Y., Li, J., Krausz, K.W., Shi, J., Brocker, C.N., Desai, D., Amin, S.G., Bisson, W.H., et al. (2015). Intestine-selective farnesoid X receptor inhibition improves obesity-related metabolic dysfunction. Nat. Commun. *6*, 10166.

9. Battle, M.A., Bondow, B.J., Iverson, M.A., Adams, S.J., Jandacek, R.J., Tso, P., and Duncan, S.A. (2008). GATA4 is essential for jejunal function in mice. Gastroenterology *135*, 1676–1686.e1. https://doi.org/10.1053/j.gastro.2008.07.074.

10. Bosse, T., Piaseckyj, C.M., Burghard, E., Fialkovich, J.J., Rajagopal, S., Pu, W.T., and Krasinski, S.D. (2006). Gata4 is essential for the maintenance of jejunal-ileal identities in the adult mouse small intestine. Mol. Cell. Biol. *26*, 9060–9070. https://doi.org/10.1128/MCB.00124-06.

11. Thompson, C.A., Wojta, K., Pulakanti, K., Rao, S., Dawson, P., and Battle, M.A. (2017). GATA4 Is Sufficient to Establish Jejunal Versus Ileal Identity in the Small Intestine. Cell. Mol. Gastroenterol. Hepatol. *3*, 422–446. https://doi.org/10.1016/j.jcmgh.2016.12.009.

12. Aliluev, A., Tritschler, S., Sterr, M., Oppenländer, L., Hinterdobler, J., Greisle, T., Irmler, M., Beckers, J., Sun, N., Walch, A., et al. (2021). Diet-induced alteration of intestinal stem cell function underlies obesity and prediabetes in mice. Nat. Metab. *3*, 1202–1216.

13. Ofengeim, D., and Yuan, J. (2013). Regulation of RIP1 kinase signalling at the crossroads of inflammation and cell death. Nat. Rev. Mol. Cell. Biol. *14*, 727–736.

14. Kelliher, M.A., Grimm, S., Ishida, Y., Kuo, F., Stanger, B.Z., and Leder, P. (1998). The death domain kinase RIP mediates the TNF-induced NF-κB. Sign *8*, 297–303.

15. Takahashi, N., Vereecke, L., Bertrand, M.J.M., Duprez, L., Berger, S.B., Divert, T., Gonçalves, A., Sze, M., Gilbert, B., Kourula, S., et al. (2014). RIPK1 ensures intestinal homeostasis by protecting the epithelium against apoptosis. Nature *513*, 95–99. https://doi.org/10.1038/nature13706.

16. Dannappel, M., Vlantis, K., Kumari, S., Polykratis, A., Kim, C., Wachsmuth, L., Eftychi, C., Lin, J., Corona, T., Hermance, N., et al. (2014). RIPK1 maintains epithelial homeostasis by inhibiting apoptosis and necroptosis. Nature *513*, 90–94. https://doi.org/10.1038/nature13608.

17. Wu, B., Qiang, L., Zhang, Y., Fu, Y., Zhao, M., Lei, Z., Lu, Z., Wei, Y.G., Dai, H., Ge, Y., et al. (2022). The deubiquitinase OTUD1 inhibits colonic inflammation by suppressing RIPK1-mediated NF-kappaB signaling. Cell. Mol. Immunol. *19*, 276–289. https://doi.org/10.1038/s41423-021-00810-9.

18. Pasparakis, M., and Vandenabeele, P. (2015). Necroptosis and its role in inflammation. Nature *517*, 311–320. https://doi.org/10.1038/nature14191.

19. Yuan, J., Amin, P., and Ofengeim, D. (2019). Necroptosis and RIPK1-mediated neuroinflammation in CNS diseases. Nat. Rev. Neurosci. *20*, 19–33. https://doi.org/10.1038/s41583-018-0093-1.

20. Patel, S., Webster, J.D., Varfolomeev, E., Kwon, Y.C., Cheng, J.H., Zhang, J., Dugger, D.L., Wickliffe, K.E., Maltzman, A., Sujatha-Bhaskar, S., et al. (2020). RIP1 inhibition blocks inflammatory diseases but not tumor growth or metastases. Cell. Death. Differ. *27*, 161–175. https://doi.org/10.1038/s41418-019-0347-0.

21. Karunakaran, D., Turner, A.W., Duchez, A.C., Soubeyrand, S., Rasheed, A., Smyth, D., Cook, D.P., Nikpay, M., Kandiah, J.W., Pan, C., et al. (2020). RIPK1 gene variants associate with obesity in humans and can be therapeutically silenced to reduce obesity in mice. Nat. Metab. *2*, 1113–1125. https://doi.org/10.1038/s42255-020-00279-2.

22. Mao, J., Hu, X., Xiao, Y., Yang, C., Ding, Y., Hou, N., Wang, J., Cheng, H., and Zhang, X. (2013). Overnutrition stimulates intestinal epithelium proliferation through beta-catenin signaling in obese mice. Diabetes *62*, 3736–3746. https://doi.org/10.2337/db13-0035.

23. Enriquez, J.R., McCauley, H.A., Zhang, K.X., Sanchez, J.G., Kalin, G.T., Lang, R.A., and Wells, J.M. (2022). A dietary change to a high-fat diet initiates a rapid adaptation of the intestine. Cell Rep. *41*, 111641. https://doi.org/10.1016/j.celrep.2022.111641.

24. Swinburn, B., Sacks, G., and Ravussin, E. (2009). Increased food energy supply is more than sufficient to explain the US epidemic of obesity. Am. J. Clin. Nutr. *90*, 1453–1456. https://doi.org/10.3945/ajcn.2009.28595.

25. Scarborough, P., Burg, M.R., Foster, C., Swinburn, B., Sacks, G., Rayner, M., Webster, P., and Allender, S. (2011). Increased energy intake entirely accounts for increase in body weight in women but not in men in the UK between 1986 and 2000. Br. J. Nutr. *105*, 1399–1404. https://doi.org/10.1017/S0007114510005076.

26. Murakami, K., Livingstone, M.B.E., Okubo, H., and Sasaki, S. (2017). Energy density of the diets of Japanese adults in relation to food and nutrient intake and general and abdominal obesity: a cross-sectional analysis from the 2012 National Health and Nutrition Survey, Japan. Br. J. Nutr. *117*, 161–169. https://doi.org/10.1017/S0007114516004451.

27. Shoelson, S.E., Lee, J., and Goldfine, A.B. (2006). Inflammation and insulin resistance. J. Clin. Invest. *116*, 1793–1801. https://doi.org/10.1172/JCI29069.

28. Hotamisligil, G.S. (2006). Inflammation and metabolic disorders. Nature *444*, 860–867.

29. Val-Laillet, D., Aarts, E., Weber, B., Ferrari, M., Quaresima, V., Stoeckel, L.E., Alonso-Alonso, M., Audette, M., Malbert, C.H., and Stice, E. (2015). Neuroimaging and neuromodulation approaches to study eating behavior and prevent and treat eating disorders and obesity. Neuroimage. Clin. *8*, 1–31. https://doi.org/10.1016/j.nicl.2015.03.016.

30. Borgstrom, B., Dahlqvist, A., Lundh, G., and Sjovall, J. (1957). Studies of intestinal digestion and absorption in the human. J. Clin. Invest. *36*, 1521–1536. https://doi.org/10.1172/JCI103549.

31. Booth, C.C., Read, A.E., and Jones, E. (1961). Studies on the site of fat absorption: 1. The sites of absorption of increasing doses of I-labelled triolein in the rat. Gut *2*, 23–31. https://doi.org/10.1136/gut.2.1.23.

32. Booth, C.C., Alldis, D., and Read, A.E. (1961). Studies on the site of fat absorption: 2 Fat balances after resection of varying amounts of the small intestine in man. Gut *2*, 168–174. https://doi.org/10.1136/gut.2.2.168.

33. Kremen, A.J., Linner, J.H., and Nelson, C.H. (1954). An experimental evaluation of the nutritional importance of proximal and distal small intestine. Ann. Surg. *140*, 439–448. https://doi.org/10.1097/00000658-195409000-00018.

34. Haber, A.L., Biton, M., Rogel, N., Herbst, R.H., Shekhar, K., Smillie, C., Burgin, G., Delorey, T.M., Howitt, M.R., Katz, Y., et al. (2017). A single-cell survey of the small intestinal epithelium. Nature *551*, 333–339. https://doi.org/10.1038/nature24489.

35. He, S., and Wang, X. (2018). RIP kinases as modulators of inflammation and immunity. Nat. Immunol. *19*, 912–922. https://doi.org/10.1038/s41590-018-0188-x.

36. Rickard, J.A., O'Donnell, J.A., Evans, J.M., Lalaoui, N., Poh, A.R., Rogers, T., Vince, J.E., Lawlor, K.E., Ninnis, R.L., Anderton, H., et al. (2014). RIPK1 regulates RIPK3-MLKL-driven systemic inflammation and emergency hematopoiesis. Cell *157*, 1175–1188. https://doi.org/10.1016/j.cell.2014.04.019.

37. Kim, Y.S., Unno, T., Kim, B.Y., and Park, M.S. (2020). Sex Differences in Gut Microbiota. World J. Mens Health *38*, 48–60. https://doi.org/10.5534/wjmh.190009.

38. Stapleton, S., Welch, G., DiBerardo, L., and Freeman, L.R. (2024). Sex differences in a mouse model of diet-induced obesity: the role of the gut microbiome. Biol. Sex Differ. *5*, 1–15. https://doi.org/10.1186/s13293-023-00580-1.

39. Martin-Sanchez, D., Fontecha-Barriuso, M., Carrasco, S., Sanchez-Niño, M.D., Mässenhausen, A.V., Linkermann, A., Cannata-Ortiz, P., Ruiz-Ortega, M., Egido, J., Ortiz, A., and Sanz, A.B. (2018). TWEAK and RIPK1 mediate a second wave of cell death during AKI. Proc. Natl. Acad. Sci. USA *115*, 4182–4187. https://doi.org/10.1073/pnas.1716578115.

40. Preeti, K., Fernandes, V., Sood, A., Khan, I., Khatri, D.K., and Singh, S.B. (2023). Necrostatin-1S mitigates type-2 diabetes-associated cognitive decrement and lipotoxicity-induced neuro-microglia changes through p-RIPK-RIPK3-p-MLKL axis. Metab. Brain. Dis. *38*, 1581–1612. https://doi.org/10.1007/s11011-023-01185-8.

41. Nik, A.M., and Carlsson, P. (2013). Separation of intact intestinal epithelium from mesenchyme. Biotechniques *55*, 42–44. https://doi.org/10.2144/000114055.

42. Love, M.I., Huber, W., and Anders, S. (2014). Moderated estimation of fold change and dispersion for RNA-seq data with DESeq2. Genome. Biol. *15*, 550. https://doi.org/10.1186/s13059-014-0550-8.

43. Bu, D., Luo, H., Huo, P., Wang, Z., Zhang, S., He, Z., Wu, Y., Zhao, L., Liu, J., Guo, J., et al. (2021). KOBAS-i: intelligent prioritization and exploratory visualization of biological functions for gene enrichment analysis. Nucleic. Acids. Res. *49*, W317–W325. https://doi.org/10.1093/nar/gkab447.

STAR★METHODS

KEY RESOURCES TABLE

REAGENT or RESOURCE	SOURCE	IDENTIFIER
Antibodies		
Mouse monoclonal anti-RIPK1	BD Biosciences	Cat#610459; RRID: AB_397832
Mouse monoclonal anti-BrdU	BD Biosciences	Cat#555627; RRID: AB_395993
Rabbit polyclonal anti-Akt	Cell Signaling Technology	Cat#9272S; RRID: AB_329827
Rabbit polyclonal anti-phospho-Akt (Ser473)	Cell Signaling Technology	Cat#9271S; RRID: AB_329825
Rabbit polyclonal anti-Villin-1	Cell Signaling Technology	Cat#2369S; RRID: AB_2215958
Mouse monoclonal β-Actin	YEASEN	Cat#30101ES; RRID: AB_3644235
Anti-mouse IgG	ZSGB-BIO	Cat#ZB-2305; RRID: AB_2747415
Anti-rabbit IgG	ZSGB-BIO	Cat#ZB-2301; RRID: AB_2747412
Chemicals, peptides, and recombinant proteins		
BrdU	Sigma-Aldrich	Cat#19-160
RIPA buffer	Solarbio	Cat#R0010
Protease inhibitor cocktail	Sigma-Aldrich	Cat#P9599
Phosphatase inhibitor	Roche	Cat#4906845001
Oil Red O Saturated Solution	Solarbio	Cat#G1260
PMSF	Solarbio	Cat#P0100
BODIPY 500/510 C1, C12 FAs	Thermo Fisher Scientific	Cat#D3823
Nec-1s	Selleck	Cat#S8641
Critical commercial assays		
TRIzol	Thermo Fisher Scientific	Cat#15596026
Cell Recovery Solution	Corning	Cat# 354253
TransScript First-Strand cDNA Synthesis SuperMix	TransGen Biotech	Cat#AT301
SuperReal PreMix Plus with SYBR Green reagent	TIANGEN BIOTECH	Cat#FP205
One Step TUNEL Apoptosis Assay Kit	Beyotime	Cat#C1089
Triglyceride assay kit	Wako	Cat#632-50991
Cholesterol assay kit	Wako	Cat#635-50981
Alanine transaminase assay kit	Roche	Cat#20764957322
Mouse Metabolic Hormone Magnetic Bead Panel (ELISA kit)	Merck Millipore	Cat#MMHE-44K
Experimental models: Organisms/strains		
Mouse: B6.Cg-Tg(Vil1-cre)997Gum/J	Jackson lab	RRID: IMSR_JAX:004586
Oligonucleotides		
Primers for *Ripk1*^{fl} allele: Forward: GCATGTTGTAACTGCCCGAC Reverse: CAGGTTGCCCTTCTCCATGT	This paper	N/A
Software and algorithms		
ImageJ	NIH	https://imagej.nih.gov/ij/
GESA	UC San Diego and Broad Institute	https://www.gsea-msigdb.org/gsea/index.jsp
R v4.0.5	R core team	https://www.r-project.org/
GraphPad Prism8	GraphPad Prism Inc	https://www.graphpad.com/
Deposited Data		
RNA-Seq data	This paper	GEO series accession: GSE282889

(*Continued on next page*)

Continued

REAGENT or RESOURCE	SOURCE	IDENTIFIER
Other		
Chow diet	Xietong Shengwu	Cat#1010002
High-fat diet	Research Diets	Cat#D12492

EXPERIMENTAL MODEL AND STUDY PARTICIPANT DETAILS

Mice

All mice procedures in this study were approved by the Institutional Animal Care and Use Committee of Peking University and were in accord with the principles of laboratory animal care of the National Academy of Sciences/National Research Council (approval number: FT-ZhangXQ-7). All mice in this study were maintained in a temperature-controlled barrier facility under specific pathogen-free conditions with a 12 h light/dark cycle and given free access to water and food in the Laboratory Animal Center (an AAALAC-accredited experimental animal facility) at Peking University, Beijing, China.

To create mice with a knock-out for IEC-specific *Ripk1*, a targeting vector was generated by inserting the genomic DNA fragment containing *Ripk1* exon 2 between the two *loxP* sites (Figure S1A). The targeting vector was linearized and electroporated into ES cells derived from C57BL/6J and 129 mixed background. Clones were analyzed for correct integration by Southern blot analysis. Chimeric mice were obtained by microinjecting the correctly targeted clones into C57BL/6 blastocysts, which then were crossed with C57BL/6 mice to obtain germline transmission. These mice were then back-crossed to C57BL/6 for at least 10 generations to obtain the *Ripk1* floxed ($Ripk1^{fl/fl}$) mice. $Ripk1^{fl/fl}$ mice were bred with *Vil*1-cre mice (purchased from Jackson Laboratory) to obtain $Ripk1^{IEC-/-}$, $Ripk1^{IEC+/-}$ mice (Figure S1B). Genotyping of the mice harboring the $Ripk1^{fl}$ allele resulted in a 484 bp fragment for the $Ripk1^{flox}$ allele and a 374 bp fragment for the WT allele (Figure S1C). Genotyping of mice expressing Vil1-Cre was performed according to the manufacturer's protocols from Jackson Laboratory.

To induce obesity, the different genotype model mice were housed separately and were fed an HFD (D12492, Research Diets, New Brunswick, NJ, USA) to 22 weeks for female mice, and 30 weeks for male mice starting at 4 weeks of age, except if noted specifically.

To test the effect of RIPK1 kinase activity on HFD-induced changes in the intestine of female mice, the RIPK1 kinase inhibitor Nec-1s was intraperitoneally injected into HFD-fed mice at dosages of 2.5 mg/kg or 5 mg/kg for 2 weeks, starting at 4 weeks of age. The dosage of Nec-1s was based on previous studies.[39,40]

METHOD DETAILS

Blood glucose, plasma insulin and ALT measurement

Blood glucose was measured by portable glucometer (Roche, ACCU-CHEK Performa) from tail vein blood. Plasma insulin was measured with an ELISA kit (Millipore, Mouse Metabolic Hormone Magnetic Bead Panel) according to the manufacturer's protocols. Plasma ALT was measured using an automatic biochemical analyzer (Roche, Cobas c311 analyzer).

Glucose tolerance test

For intraperitoneal glucose tolerance test (ipGTT), mice were fasted for overnight, then glucose was injected intraperitoneally at 2 g/kg body weight. Blood samples were taken from the tail vein at the indicated time points and glucose levels were measured by a portable glucometer.

Lipid absorption assay

Mice were fasted overnight and then 10 mL/kg of olive oil was gavaged orally. Plasma samples were obtained from the tail vein before and 1, 2, and 4h after the fat challenge to determine plasma lipid levels. Plasma total cholesterol (LabAssay Cholesterol, Wako) and triglycerides content (LabAssay Triglyceride, Wako) were measured according to the manufacturers' protocols.

In an alternative assay, mice were fasted for 4 h and gavaged with BODIPY 500/510 C1, C12 FAs (2 μg/g body weight; Molecular Probes #D3823), and olive oil (10 μL/g bodyweight). The mice were euthanized 2 h after gavage. Their small intestines were excised and embedded in Tissue-Tek O.C.T. Compound (Sakura Finetek, Torrance, CA, USA). 10 μm sections were prepared and mounted with DAPI, and the sections were imaged under a fluorescence microscope. For quantitative analysis, lipid droplet area was measured within 50 well-oriented villi using ImageJ (NIH, Bethesda, MD).

Tissue sample collection

To evaluate intestinal epithelial cell proliferation, BrdU (Sigma, St. Louis, MO) at 100 mg/kg body weigh was injected into the mice intraperitoneally, and the mice were anesthetized and killed by cervical dislocation 1 h after the injection. To evaluate insulin sensitivity, the mice were euthanized 15 min after injecting insulin into the peritoneum (1 U/kg body weight). Blood was collected, and the plasma was separated by centrifugation. Small intestinal and other tissues were harvested for further study. To collect different parts

of the intestine, the entire intestine was removed and rinsed rapidly in ice-cold ringer buffer (115 mM NaCl, 25 mM $NaHCO_3$, 1.2 mM $MgCl_2$, 1.2 mM $CaCl_2$, 2.4 mM K_2HPO_4, and 0.4 mM KH_2PO_4, pH 7.35) supplemented with phenylmethylsulfonylfluoride. The rinsed small intestines were cut into three segments with length ratios of 1:3:2 (corresponding to duodenum, jejunum, and ileum), and rapidly frozen in liquid nitrogen for RNA or protein extraction, or fixed in 4% paraformaldehyde (PFA) for histological and immunohistochemical analysis. The intestinal epithelium and muscle layer were separated as in a previous report.[41] Briefly, the intestinal segments were flushed with ice-cold ringer buffer and inverted for a thorough wash. The intestines were then incubated in 5 mL of ice-cold Cell Recovery Solution for 40 min to allow epithelium detachment. The separated epithelium and muscle layer were collected in separate tubes, centrifuged at 5000g for 5 min, and snap frozen in liquid nitrogen for protein extraction. For Oil red O staining, a small piece of the liver was embedded in Tissue-Tek O.C.T. Compound. for make frozen sections later.

Histology and immunohistochemistry

Tissues fixed in PFA were embedded in paraffin, and 3–5 μm sections were prepared. The sections were stained with hematoxylin-eosin (HE) for histological analysis. For immunohistochemistry, sections were incubated with anti-BrdU (BD, 1:600), anti-CC3 (CST, 1:400) or anti-CD45 (abcam, 1:100) antibodies overnight at 4°C, followed by incubation with anti-mouse (Dako Diagnostics, 1:1000) or anti-rabbit (ZSGB-BIO, PV-6001) horseradish peroxidase–labeled secondary antibodies for 1 h at room temperature. Slides were developed using 3,39-diaminobenzidine tetrahydrochloride and counterstained with hematoxylin. Sections were imaged under a microscope (IX73, Olympus). For quantitative analysis, BrdU-positive cells were imaged within 50 well-oriented crypts from ten 20× images and counted per crypt using ImageJ (NIH, Bethesda, MD).

For immunofluorescent staining, sections were incubated with anti-RIPK1 (BD, 1:600) antibody overnight at 4°C, followed by incubation with Alexa Fluor 568 goat anti-mouse IgG(H + L) (Invitrogen, 1:1000) for 1 h at room temperature. Images were taken by fluorescent microscope (Leica, DM4B).

TUNEL staining

To detect cell death *in situ*, TUNEL staining of paraffin sections was performed using a One Step TUNEL Apoptosis Assay Kit (C1089, Beyotime) following the manufacturer's instructions. TUNEL-positive cells were imaged under the same microscope. For quantitative analysis, TUNEL-positive cells from ten 20× images were counted using ImageJ (NIH, Bethesda, MD).

Western blotting

Intestinal tissues were homogenized and lysed by RIPA buffer (Solarbio, R0010) supplemented with a protease inhibitor cocktail (1:100, Sigma), a phosphatase inhibitor (1:10, Roche), and 2 mM PMSF. Protein lysates were analyzed by 10% SDS-PAGE, and transferred to a PVDF membrane (Millipore). After the protein bands were transferred, the membranes were blocked in 5% fat-free milk at room temperature for 1 h, and the membranes were incubated at 4°C overnight with the following primary antibodies: anti-RIPK1 (1:1000, BD), anti-AKT (1:1000, Cell signaling), anti-*p*-AKT (Ser473,1:1000, Cell signaling), anti-villin1 (1:1000, Cell signaling), anti-β-actin (1:1000, Yeasen Biotechnology), followed by a 1-h incubation with anti-rabbit or mouse horseradish peroxidase–labeled secondary antibodies (1:2000, ZSGB-BIO) at room temperature. An ECL detection system (Bio-Rad) was used to reveal the peroxidase label. Relative abundance was quantified by densitometry using ImageJ.

RNA-seq analysis

Total RNA of duodenum, jejunum or ileum extracted by a TRIzol Reagent (Thermo Fisher Scientific, 15596026) were subjected to RNA-Seq analysis on a DNBSEQ2000 system in the Beijing Genomics Institute (BGI), China. RNA quantification and quality assessment were performed with the Agilent 2100 Bioanalzyer. After library construction, paired-end 150 base pair reads were generated on the DNBseq platform. The raw file (fastq) was processed to quality check, alignment, sorting and annotation by using viz. FastQC, Bowtie2, HISAT2, and Samtools along with imperative files containing the mouse genome reference sequence (GRCm39 from UCSC genome browser on mouse) and genes coordinate information file. Gene expression levels (TPM) were calculated from gene reads. After performing pre-filtering to keep only rows that have an average count of at least 1, differentially expressed genes (DEG) were analyzed by DESeq2[42] using a fold-change (FC) > 2 and a adjusted *p*-values cut-off <0.05. GSEA software and KOBAS[43] were used to analyze functional and pathway enrichment, respectively.

Screening signature genes

We defined the signature genes according to the method in previous studies.[11] Differential genes between groups were screened using a 2-fold change and a adjusted *p* value less than 0.05 as the threshold. Briefly, differential genes were screened in duodenum and jejunum, jejunum and ileum, and duodenum and ileum, respectively, following the thresholds above. The set of genes that were significantly higher in duodenum than in jejunum and ileum was defined as the signature genes of duodenum. The set of genes that were significantly higher in jejunum than in duodenum and ileum was defined as the signature genes of jejunum. The set of genes that were significantly higher in ileum than in duodenum and jejunum were defined as the signature genes of ileum. The set of genes that were not significantly different between duodenum and jejunum but significantly higher than ileum was defined as the signature gene of duodenum-jejunum.

qRT-PCR analysis

Total RNA was extracted from intestine tissues using TRIzol Reagent (Thermo Fisher Scientific, 15596026). cDNA was prepared with TransScript First-Strand cDNA Synthesis SuperMix (TransGen Biotech, AT301) according to the manufacturer's protocols. qRT-PCR was performed to analyze the expression of target genes on a CFX96 Touch Real-Time PCR Detection System (BIO-RAD) using SuperReal PreMix Plus with SYBR Green reagent (TIANGEN BIOTECH, FP205) with the primer sets (Table S2), *Actb* was used as the reference gene.

QUANTIFICATION AND STATISTICAL ANALYSIS

All data are expressed as mean ± SE, unless otherwise indicated. Statistical analysis was performed by using the unpaired *t*-test or ANOVA with GraphPad PRISM version 8.0 (GraphPad software, Inc.). p value <0.05 was considered statistically significant. The western blotting quantifications were conducted in ImageJ (NIH, USA). Animals were randomly assigned to experimental groups. The number of animals per experimental group is presented in each figure and figure legends.